Available online at www.sciencedirect.com
SCIENCE DIRECT
Polymer 46 (2005) 827–844
polymer
www.elsevier.com/locate/polymer

Filler toughening of plastics. Part 1—The effect of surface interactions on physico-mechanical properties and rheological behaviour of ultrafine $CaCO_3$/HDPE nanocomposites

A. Lazzeri[a,*], S.M. Zebarjad[b], M. Pracella[c], K. Cavalier[d], R. Rosa[d]

[a]*Center for Materials Engineering, University of Pisa, Via Diotisalvi 2, 56126 Pisa, Italy*
[b]*Department of Materials Science and Engineering, Ferdowsi University, Mashhad, Iran*
[c]*CNR, Institute for Biomedical and Composite Materials, Section of Pisa, Via Diotisalvi 2, 56126 Pisa, Italy*
[d]*Solvay SBU Advanced Functional Minerals, PCC Research Center for Polymers, Plastisols and Sealants, 13129 Salin de Giraud, France*

Received 17 October 2004; received in revised form 29 November 2004; accepted 30 November 2004
Available online 19 December 2004

Abstract

Precipitated $CaCO_3$ (PCC)/High Density Polyethylene (HDPE) composites were prepared on a twin screw mixer-single screw extruder with a particle content of 10 vol%. The average particle size was 70 nm. The influence of surface treatment of the particles, with and without stearic acid (SA), on the physico-mechanical and rheological properties was studied. The experiments included tensile tests, impact tests, differential scanning calorimetry (DSC), microscopy and rheology experiments. The addition of 10 vol% calcium carbonate to HDPE causes a rise in Young's modulus and yield stress of its composites and is accompanied by a sharp drop in impact strength. The addition of SA has the effect of slightly decreasing both Young's modulus and yield stress of the composites compared to the uncoated PCC composites, while the impact strength progressively increases.

During the tensile test filled HDPE composites showed stress whitening zones appear and develop along the gauge length. Volume measurements during tensile tests showed an increase in volume strain with deformation, due to the matrix-particle debonding phenomenon, while pure HDPE showed actually a decrease in volume with elongation. At constant deformation, for the composites with coated PCC, it can be observed that an increase in the SA content leads to a slight decrease in volume change. The microscopical evaluation showed cavities and voids due to debonding and deformation bands in the stress whitened areas.

DSC experiments have shown that uncoated PCC particles have a very small nucleating effect on HDPE.

Keywords: Nanocomposites; Filler toughening; Surface agents

1. Introduction

The toughness of both commodity and engineering plastics at extreme conditions such as impact loading and low temperatures can be improved by means of the incorporation of rubber particles, albeit at the expense of a reduction in the elastic modulus of the material [1]. The use of rigid fillers to toughen polymers has also received considerable attention in recent years [2–9]. This approach would, in principle, lead to rigid and tough composites. An early paper reported toughening of isotactic polypropylene (iPP) using ultrafine calcium carbonate (average particle size 70 nm) [9]. In that work, the use of nanosized particles, suggested by the concept of a critical interparticle distance [10], could obtain a limited increase in fracture toughness, attributed to crack-pinning [11–14], while at higher filler loadings a good dispersion of the particles was not achieved. At the time when that early paper [9] was written, a thorough understanding of the principles governing toughening of polymers was still lacking.

Recently Lazzeri and Bucknall have elucidated the mechanism for rubber toughening in non-crazing polymers [15–17]. They showed that these particles can facilitate the

* Corresponding author. Tel.: +39 050 511207.
E-mail address: a.lazzeri@ing.unipi.it (A. Lazzeri).

0032-3861/$ - see front matter © 2004 Published by Elsevier Ltd.
doi:10.1016/j.polymer.2004.11.111

development of microvoids and activate dilatational yielding in the deformed zone close to the fracture surface.

Similar to the requirement of void creation via cavitation in the rubber toughening mechanism, Argon and Cohen proposed that for toughening to occur in rigid filler systems, the particles must debond from the matrix, creating voids around the particles and allowing the interparticle ligaments to deform plastically [4–7]. In fact, the stretching of the matrix ligaments between cavitated or debonded particles is the main adsorbing energy mechanism. On the other hand, voids reduce the macroscopic plastic resistance of the material and void coalescence also potentially decreases the fracture strain and the overall toughness achievable by the material. Ideally, the voids should not form immediately upon application of stress as this may reduce the elastic modulus[1].

So to improve toughness, it is necessary to obtain a low particle matrix adhesion (to favour debonding) but at the same time it is also necessary to prevent particle agglomeration and void coalescence. The two conditions are often contradictory, in the sense that when the adhesion between a second phase particle and the matrix is weak, agglomeration is most often observed, while a strong adhesion, although enabling to achieve a uniform dispersion, almost inevitably leads to a lack of debonding and brittle behaviour. The problem is even more difficult to be solved since, to minimise the negative effects of void coalescence, very fine particles are to be used. Because of their small size, these particles show a strong tendency to agglomerate.

Thus the challenge is to find a suitable surface agent that can reduce the surface tension between the inorganic particles and the polymer matrix, thus enabling to obtain a good dispersion, but, on the same time, being able to disentangle rapidly from the interphase region between the filler and the polymer allowing for easy debonding and prompt microvoid formation.

Recently a few papers have reported toughening of polyethylene and polypropylene with small $CaCO_3$ particles coated with stearic acid (SA) [5,7–9,18]. These studies found an optimum particle size of about 0.7 μm, with smaller particles failing to bring about high levels of toughness due to particle coalescence. It is our opinion that this behaviour is caused by an 'imperfect' coating of the particles. This is typical of commercial Precipitated Calcium Carbonate (PCC) powders where the level of surfactant is well below that required for a monolayer coating.

[1] A rather similar concept had been suggested earlier by Fu and Wang [8] although the principles of filler toughening were not as clearly formulated. In fact these authors correctly pointed out the issue of debonding and stretching of the interparticle ligaments to achieve high toughness, but they suggested a high interfacial adhesion as necessary to achieve the fine filler dispersion required for rigid inorganic toughening. This is the main point of divergence of our approach with that proposed in [8].

The focus of this study is on the determination of the optimum surfactant content in order to achieve tough PCC/HDPE nanocomposites, as a first example of the applications of these new ideas to filler toughening. The reason for choosing calcium carbonate is because it is the most widely used filler for plastics and it can be used at high loading. It is available in different grades: dry processed, wet or water ground and can be easily surface treated. PCCs can be produced in three polymorph forms (vaterite, aragonite or calcite) of $CaCO_3$ and a wide variety of particle sizes and shapes, including plates and acicular forms. However, only the calcite form with a rhombohedric cell and a low aspect ratio has found much commercial application in polymers. For filler applications the particles have an ultimate particle size of 50–100 nm with a corresponding specific surface area of 15–25 m^2/g. The particles have an aspect ratio close to one, so reducing the stress concentration and, therefore, the risk of void coalescence after debonding from the matrix.

From the perspective of toughness enhancement, SA and other fatty acids, probably the most largely used surface treatment systems for particulate mineral fillers, are the best candidates since they can improve filler dispersion with the advantage of low filler–matrix interaction. These surfactants have one polar group and a long aliphatic chain, which can reduce the surface tension between a non-polar, hydrophobic polymer like HDPE and the polar hydrophilic calcium carbonate particles. Rothon [2] distinguishes surface modifiers in 'coating agents' and 'coupling agents'. With the first class of surface agents, the filler surface is rendered more hydrophobic and thus more compatible with the polymer, while, with the second approach, coupling agents form strong bonds between the filler and the matrix.

From the point of view of filler toughening, coupling agents are not to be used since, even if they lead to a good dispersion and strong increases in both yield stress and Young's modulus, this is associated with a general reduction of fracture resistance. On the other hand, coating agents also enable to reach a good level of dispersion but allow debonding to take place followed by matrix dilatational yielding. This is accompanied to enhanced fracture toughness at the expenses of a more limited increase in stiffness and, quite often, a reduction in yield stress. This aspect is often misunderstood in the scientific and technical literature and stearic acid and other coatings are often accounted for as coupling agents since the addition of both types of surfactants can be associated with improvements in filler dispersion.

According to Osman and Suter, stearic acid reacts with the surface of $CaCO_3$ forming calcium stearate bicarbonate [19]. The SA aliphatic tail is virtually a very short segment of polyethylene, so it is predictably fully compatible with the bulk polymer, but its length is too short to form entanglements with the matrix chains. Theoretically, SA molecules lie perpendicular to the filler surface to form a closely packed layer with a thickness of about 2.5 nm,

which corresponds to their fully extended chain length [2]. SA coating substantially reduces the surface tension of PCC particles from 210 mJ/m^2 to 40–60 mJ/m^2 [20], below the level for polymer/polymer interaction which is of the order of 65 mJ/m^2 [21–22]. Filler treatment with SA results in a coating that renders the filler surface hydrophobic without forming strong bonds between the filler and the polymer.

However, to the aim of toughness improvements, the determination of the optimum amount of coating is a critical factor for the efficiency of the treatment. It depends on the type of the interaction, the size of the treating molecule, its alignment to the surface and on some other factors. An insufficient amount of SA is associated with particle agglomeration, while excessive quantities may bring to processing problems as well as to the deterioration of mechanical properties and appearance of the product [2–3, 23].

The aim of this research is to determine the effect of SA on the physical, rheological and mechanical properties of PCC/HDPE composites with a special regard to impact strength. The results are presented in a two-part paper. The approach followed is that of trying to elucidate the effects of interfacial interactions on physical and mechanical properties of the composites by varying the levels of surface coverage. Part 1 discusses the results of calorimetric and rheological analysis, together with the results of impact tests and tensile tests with measurement of volume changes carried out on a series of PCC/HDPE composites with varying degree of SA coating on the particles. Part 2 considers the fracture mechanics characterisation of the impact behaviour in relation to the morphology of the fracture surface and to the degree of dispersion of the particles in the matrix.

2. Experimental procedure

2.1. Materials

High density polyethylene (HDPE) Eltex B4020 from Solvay Polyolefins, Rosignano, Italy was used. The filler particles were SOCAL® PCC obtained from Solvay SBU Advanced Functional Minerals, Salin de Giraud, France.

Two different series of PCC particles have been used in this work. In the present paper, a series of 10 different powders has been used with a SA content varying from zero to a maximum of 9% by weight (see Table 1). Since the SA content corresponding to the theoretical monolayer concentration of SA is around 5 wt% for this particle size, the SA/theoretical monolayer coating ratio varies from 0 to about 1.7. The PCC powders in this series, at each different SA coating level, showed a slightly different average particle size varying in the range 56–72 nm and a corresponding specific surface spanning from 16 to 22 m^2/g (see Table. 1). These materials have been used to evaluate the effect of surface agent treatment on thermal properties and on the tensile and volume change behaviour of PCC/HDPE composites, where it has been checked that particle size has not a major role on the observed performance, in the experimental conditions considered.

For each type of particles, a volume fraction of 10% was used for the preparation of the composites.

For the work described in the next paper, a second series of particles has been prepared by Solvay Advanced Functional Minerals, with a SA coating up to a maximum of 13.5% by weight and a controlled average size of approximately 62 nm. These materials have been used to determine the impact properties of PCC/HDPE composites, since particle size is critical in determining fracture toughness.

2.2. Sample preparation

Before mixing, PCC powders were dried under vacuum condition for a minimum of 8 h. Oven-dry PCC powders and HDPE pellets were first mechanically mixed to achieve HDPE/10 vol% $CaCO_3$ composites. The general code was PExx with xx the nominal amount of SA in g/kg of PCC. Table 2 provides details of the composition of each blend studied in this work. Moreover, Table 1 reports the corresponding effective total organic content (MOT) measured by gravimetry for all powders. The mixtures were fed into a two stage processing unit composed by a twin screw non-intermeshing corotating mixer (COMACPLAST, Milano) and a MV45 single-screw extruder (COMACPLAST, Milano) with 45 mm diameter, length/diameter ratio 28:1 and were extruded under the condition of Table 3. Unfilled HDPE was also similarly processed, first in the twin screw non-intermeshing corotating mixer followed by a passage in the single-screw extruder, to ensure analogous process conditions and thermomechanical history for all composites since processing-induced microstructural changes are well known for polyolefins, see for example Ref. [21]. All extruded materials were cooled in water at room temperature. The resultant composite pellets were then granulated by a milling device before moulding.

2.3. Mechanical probes

Tensile specimens were produced using an OIMA-85 ECO 3080 injection moulding machine c/o Interplast, Scandicci (FI), Italy, under the conditions described in Table 4. The injection moulded specimens were coded according both to the SA content and PCC volume fraction.

2.3.1. Tensile response and dilatometry tests

ASTM D638 Type I dog-bone tensile bars of HDPE and its composites were moulded with nominal gauge length of 50 mm, width of 12.7 mm, and thickness of 3.2 mm. Tensile dilatometry tests were carried out with an Instron 1430 tensile tester, following the ASTM D638 procedure, at a crosshead speed of 10 mm/min which corresponds to a

Table 1
Specification of PCC powders

Material	BET surface (m^2/g)	Nominal SA/PCC weight ratio (g acid/kg PCC)	MOT measured by gravimetry (g acid/kg PCC)	SA surface concentration (mg/m^2)
PCC00	16.0	0	0	0
PCC20	16.0	20	23.7	1.48
PCC30	19.0	30	33.8	1.78
PCC38	19.0	38	40.7	2.14
PCC45	16.0	45	46.3	2.89
PCC50	22.1	50	51.0	2.30
PCC55	21.8	55	58.0	2.66
PCC60	21.7	60	62.0	2.86
PCC70	21.5	70	72.0	3.34
PCC90	21.3	90	92.0	4.32

strain rate of 0.4 min^{-1}. At least three samples for each material were tested at room temperature. The Instron was connected to a computer for data collection and analysis. Elongation and specimen width were measured during deformation using two extensometers, one along the tensile direction (axial) and the other perpendicular to it (lateral). By assuming the two lateral strain components to be equal [24], the volume strain is then given by:

$$\frac{\Delta V}{V_o} = (1+\varepsilon_1)(1+\varepsilon_2)^2 - 1 \quad (1)$$

where ΔV is the change in volume, V_o the original volume, ε_1 the axial strain, and ε_2 the lateral strain.

Volume strain is measured with two extensometers assuming that the changes in the thickness and width are the same, the sample cross section remains rectangular and the deformation is affine (non-necking in the measured zone).

In order to assure the validity of the results, care was taken to check the validity of these assumption and to record when, during the test, the deformation ceased to be homogeneous throughout the specimen (i.e. the sample formed a neck). In fact, the necking phenomenon was observed in both pure HDPE and its composites at about 30% elongation. Until this point the measurements of volume changes were possible. No evidence of differential changes in width and thickness were noticed. Also the cross section appeared to keep its rectangular shape during straining.

Table 2
Specification of materials used

Material	HDPE Volume content (%)	PCC Volume content (%)	Nominal SA/PCC weight ratio (g acid/kg PCC)
Pure HDPE	100	0	–
PE00	90	10	0
PE20	90	10	20
PE30	90	10	30
PE38	90	10	38
PE45	90	10	45
PE50	90	10	50
PE55	90	10	55
PE60	90	10	60
PE70	90	10	70
PE90	90	10	90

A minimum of three samples for each material were tested at room temperature at a crosshead speed of 10 mm/min which corresponds to a strain rate of 0.4 min^{-1}.

2.4. Impact tests

To evaluate the impact strength of the materials, impact tests were carried according to ASTM D256, using a CEAST (Torino, I) pendulum with a striking speed of 3.5 m/s. A minimum of five specimens were tested and the average energy was calculated for each point reported.

2.5. Calorimetric analysis

In order to investigate the thermal properties of HDPE and its composites, a calorimetric analysis was carried out. A Perkin–Elmer DSC-2C differential scanning calorimeter equipped with Data Station 3600 was used to analyse samples cut from injection moulding specimens. All measurements were performed under nitrogen flow. The mass of the samples used varied between 5 and 9 mg. The samples were put in an aluminium crucible and crimped using a small press. The analysis was carried out according to the temperature program shown in Fig. 1. The samples were first heated at a rate of 10 °C/min from 30 °C to above 200 °C and held at this temperature for about 5 min. The samples were then cooled to room temperature at 10 °C/min. A second heating run was performed at the same rate through the full melting range. Indium was employed as a standard for temperature and enthalpy calibration of DSC.

The melting temperature (T_m) and the crystallization temperature (T_c) of polymer were recorded at the maximum of the melting peak and to the minimum of the crystallization peak, respectively. The onset crystallization temperature (T_O) was determined at the beginning of the crystallization peak (at the intersection of the peak slope with the baseline). The heats of melting (ΔH_m) and crystallization (ΔH_c) were determined from the corresponding peak areas in the heating and cooling thermograms.

The percent crystallinity of HDPE in the composites

Table 3
Extrusion conditions

Speed (rpm)		Temperature in different zones (°C)				
Mixer	Extruder	Zone I	Zone II	Zone III	Zone IV	Zone V
200	60	160	165	175	185	200

were calculated as follows:

$$X_C(\text{HDPE}) = \frac{\Delta H(\text{Composite})}{\Delta H^0 \times W(\text{HDPE})} \quad (2)$$

Where ΔH (composite) is the apparent enthalpy of fusion per gram of composite, ΔH^0 (HDPE) is the heat of fusion of 100% crystallinity HDPE, taken as 293 J/g from [25], and W (HDPE) is the weight fraction of HDPE in the composites.

2.6. Viscometry

Viscometry tests have been performed employing a Rheovis capillary viscometer, (CEAST, Torino, Italy). In this experiment, the piston force, its speed, the shear stress, strain and viscosity are monitored as functions of time at a temperature of 200 °C. The cylinder and the capillary have a diameter of 9.55 mm and 1 mm, respectively, and a length of 40 mm, so that the capillary length–diameter ratio, L/D = 40. The cylinder was kept at a temperature of 200 °C, the cylinder was filled with the polymer and compressed to remove the trapped air. The piston speed was kept at 0.0139, 0.0693, 0.1385, 0.2078, 0.4155, 0.6, 1 e 1.5 mm/s during the experiments.

2.7. Morphological analysis

To clarify the mechanism of deformation, after testing, some samples were cold fractured along the tensile direction. The new fracture surfaces have been subsequently investigated by scanning electron microscopy. A Jeol JSM-5600LV scanning electron microscope was used to study the side surfaces of tensile bars and fracture surface of selected samples. The specimens were coated, by using a sputter coater Edward S150B, with a thin layer of gold prior to microscopy to avoid charge build up.

3. Experimental results

3.1. Tension tests

Fig. 2 shows stress-strain curves for pure HDPE and its composites. The stress-strain curves exhibited a maximum at a certain deformation associated with yielding. As it is seen, addition of 10 vol% PCC and SA does not qualitatively change the mechanical behaviour of the materials.

Fig. 3 presents the dependency of yield stress from the SA surface concentration in 10 vol% PCC/HDPE composites. As it can be seen from the graph an addition of 10 vol% of calcium carbonate to HDPE causes a rise in yield stress in all composites, as reported earlier in the literature [8], but the value of yield stress decreases with increasing the SA content. From a careful examination of the data in Fig. 3, it appears that the reduction is continuous until a plateau level is attained, from a SA surface concentration of about 2.7 mg/m^2. This can be interpreted as the result of a decreased strength of the interphase layer between the polymer and the filler particles, due to the reduced level of interaction by increasing the quantity of coating. In the case of the uncoated filler, due to its high surface area, adsorption of HDPE molecules is likely to occur, leading to a rigid interphase. In contrast, the progressive addition of SA to the surface of the PCC particles should reduce the stress transfer ability of the interphase and even its thickness, leading to a softer interphase.

Reduction of yield stress on increasing $CaCO_3$ content in polyolefins is reported by several investigators [26–28], while a reduction of yield stress with SA content in $CaCO_3$/polyolefin composites is also reported by some investigators [27–28]. The main difference between our work and those reported in the literature is the filler particle size.

Fig. 4 shows the variation of Young's modulus of 10 vol% PCC/HDPE composites versus real SA surface concentration. As it is seen, addition of 10 vol% uncoated PCC causes a 70% rise in Young's modulus and about 45% for coated PCC. As observed for the yield stress, increasing the SA content leads to a progressive decrease in Young's modulus until a plateau value is reached. Again this can be explained in term of a progressively softer interphase which forms upon increasing the SA content.

Table 4
Injection moulding conditions

Pressure (bar)		Temperature zones (°C)			Mould temperature (°C)
First	Second	Zone I	Zone II	Zone III	
95	100	260	270	290	50

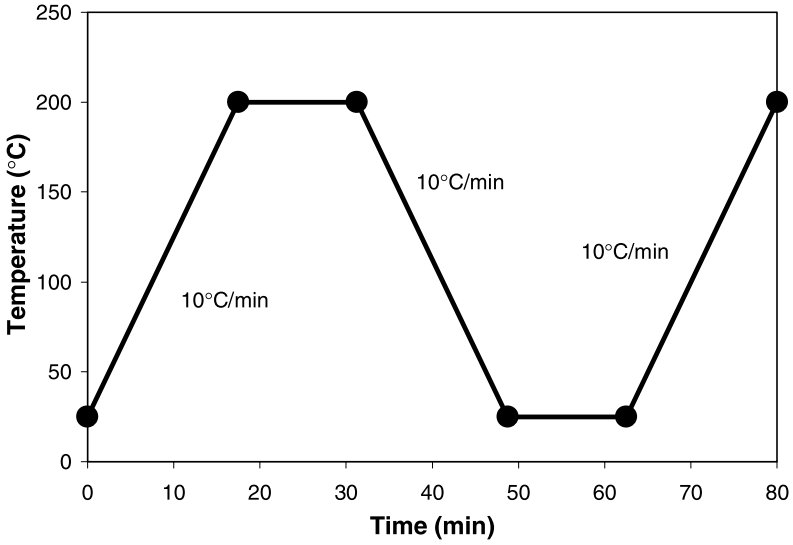

Fig. 1. Temperature program for calorimetric analysis.

3.2. Tensile dilatometry

The volume strain versus longitudinal strain for neat HDPE and its composites are shown in Fig. 5. For all materials, except for pure HDPE, it can be observed an increase of volume strain with deformation[2].

The decrease of volume strain with deformation for pure HDPE is probably due to the fact that the stretching of non-crystalline (rubbery) phases leads to the orientation of the amorphous chains parallel to each other to form a kind of mesomorphic structure similar to those found in liquid–crystal polymers in the smectic state, with a consequent decrease in volume strain, as suggested by Gaucher-Miri et al. [30]. The decrease in volume strain on stressing pure HDPE could also be due to further crystallization. The investigation over the reasons leading to a negative volume strain in HDPE is beyond the scope of the present work and will be a task postponed to a future research effort.

The presence of $CaCO_3$ particles has the opposite effect causing an increase of volume strain due to the debonding phenomenon. To highlight the effects of particle–matrix debonding and the consequent increase in volume due to void growth and coalescence, it is preferable to separate the effects of the volume evolution of the matrix polymer in the composite.

In the hypothesis that the only contributions to volume due to the presence of the particles are given by void nucleation at the matrix–filler interface followed by the void growth and coalescence, while the matrix contribution to volume is not affected by the presence of the filler, the

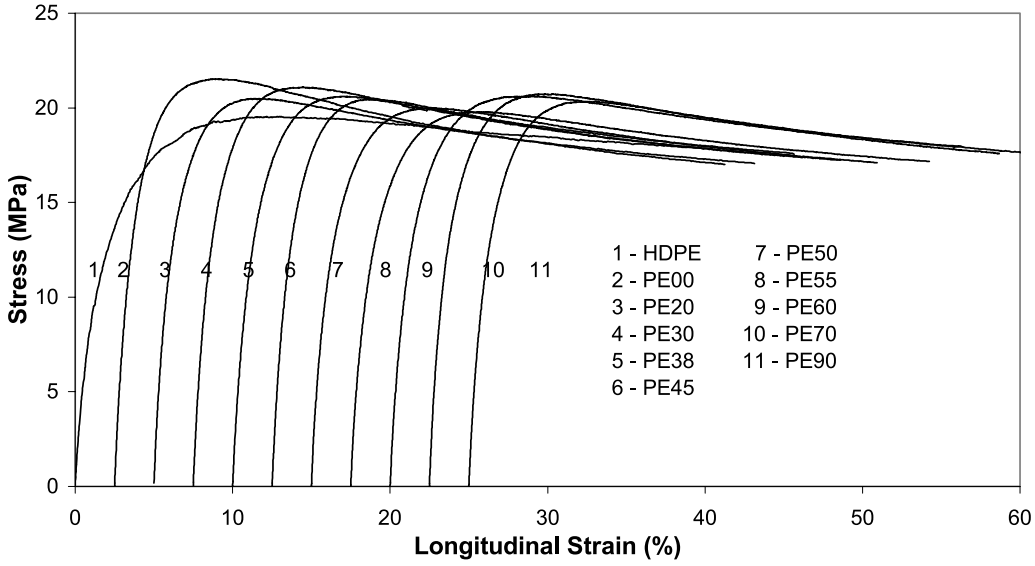

Fig. 2. Stress–strain curves for pure HDPE and its composites at 0.2 min^{-1} strain rate. Curves 2–11 have been shifted of a factor 2.5% along the longitudinal strain axis for clarity.

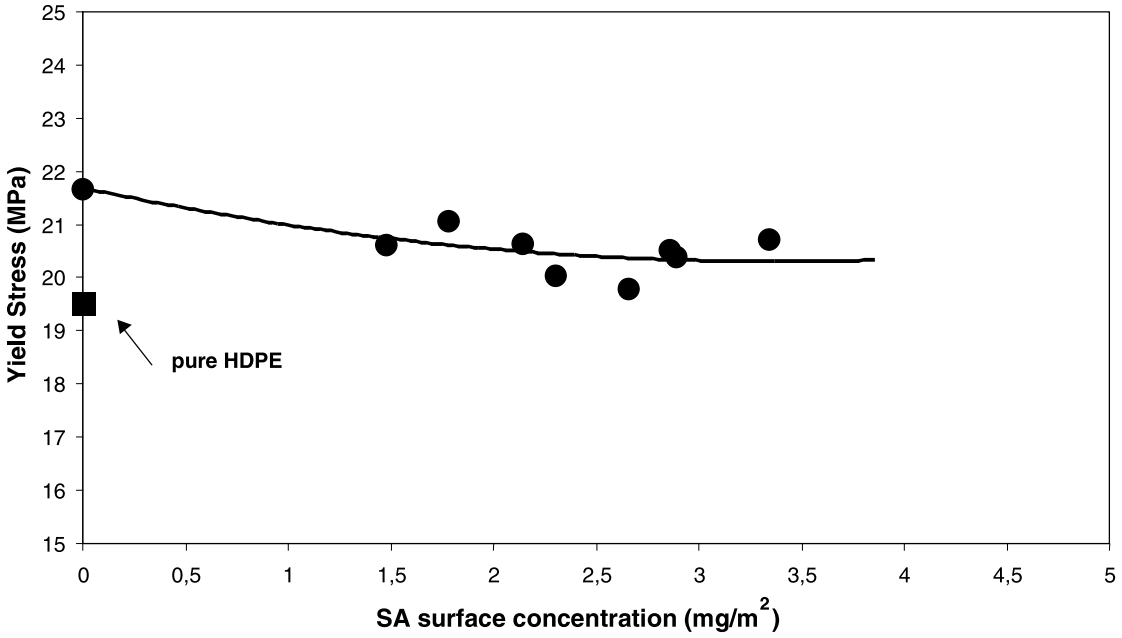

Fig. 3. Dependency of yield stress from SA content in 10 vol% PCC/HDPE composites.

overall volume strain of the composite can be represented with the following equation [31]:

$$\left(\frac{\Delta V}{V_0}\right)_C = \left(\frac{\Delta V}{V_0}\right)_M (1-\varphi) + \left(\frac{\Delta V}{V_0}\right)_V \quad (3)$$

where $(\Delta V/V_0)_c$ is the volume strain of a composite as measured, $(\Delta V/V_0)_M$ the volume strain of the matrix component in the composite, ϕ the filler volume fraction, $(\Delta V/V_0)_V$ the volume strain due to debonding, void growth and coalescence. In Eq. (3), $(\Delta V/V_0)_M$ is taken to be a function of strain only; furthermore, it is not necessarily the same as the volume strain of the unfilled HDPE.

Eq. (3) can be recast in the following form:

$$\left(\frac{\Delta V}{V_0}\right)_V = \left(\frac{\Delta V}{V_0}\right)_C - \left(\frac{\Delta V}{V_0}\right)_M (1-\varphi) \quad (4)$$

The $(\Delta V/V_0)_V$ value, calculated from Eq. (4), is plotted versus axial strain in Fig. 6 for PE00 and PE50. In the calculation of $(\Delta V/V_0)_V$ we have made the assumption that $(\Delta V/V_0)_M$ is the volume strain of the unfilled HDPE, i.e. that

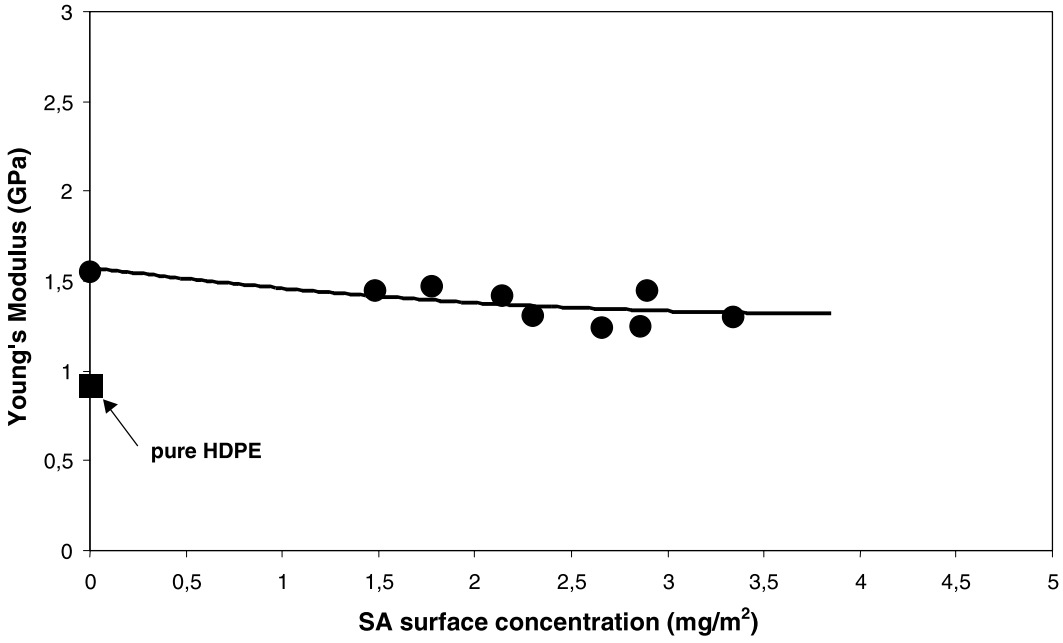

Fig. 4. Variation of Young's modulus of 10 vol% PCC/HDPE composites versus SA content.

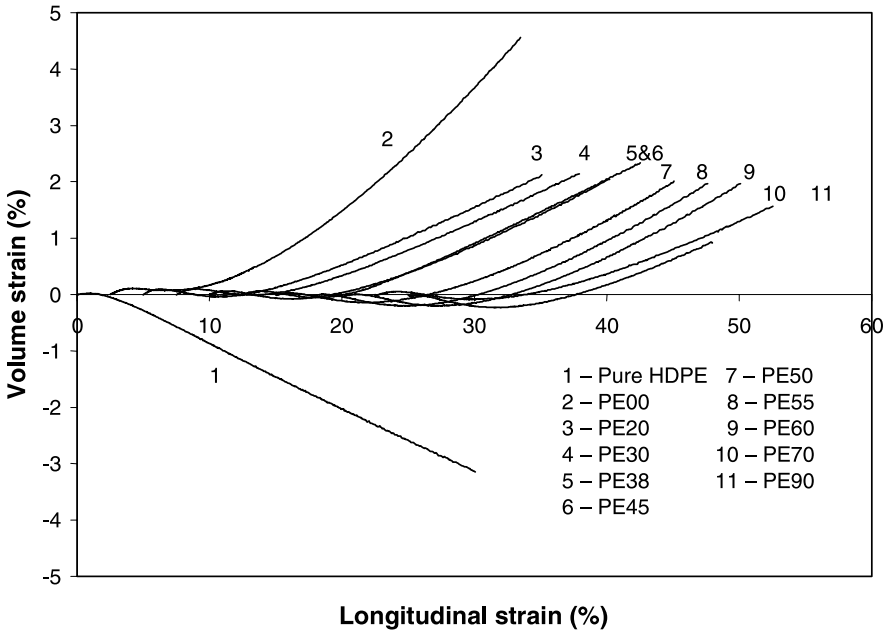

Fig. 5. Volume strain versus longitudinal strain for neat HDPE and its composites. Curves 2–11 have been shifted of a factor 2.5% along the longitudinal strain axis for clarity.

the volume strain behaviour of the matrix in the composite was the same of pure HDPE.

These curves show the extent of the volume evolution due to the debonding phenomenon. For all composites debonding takes place at deformation level of the order of 2%, although in presence of SA the slope of the volume change versus elongation curve is much lower. Above 20% strain the volume evolution appears to be a linear function of the longitudinal strain. Extrapolation of the linear part of the volume strain curve to $\Delta V = 0$ gives a value of about 9% strain, irrespective of SA content.

Fig. 7 shows the dependency of ΔV of the composites as a function of the SA content/m^2 of PCC for value of deformation of 2, 5 and 8%. As it can be seen the addition of SA causes a continues decrease in ΔV with respect to the value of the HDPE/uncoated PCC. Incidentally we note a slight drop when the volume strain for the particles with nominal stearic acid content from 2% to 4.5% is compared to that measured for those with SA content from 5% to 9%. The reason might be associated to the slight difference in particles size between these two series of particles, reflected from their value of BET surface. Particle size effects on the observed volume strain during tensile tests were in fact reported in [31]. These effects appeared to be novel and a tentative explanation was given in [31] assuming the existence of a 'tied or confined amorphous' layer whose molecular mobility is reduced. This immobilized layer of polymer on the surface of the filler particles causes debonding to occur not directly at the particle surface but at a weaker interface between the immobilized layer and the matrix. The overall effect, in terms of volume evolution, is to increase the effective volume fraction of the particles due to the addition of the immobilized layer. The explanation given in [31] can also shed some light also on the results presented in this work. In fact, as stated above, the progressive addition of SA to the surface of the PCC particles should lead to a softer interphase with a reduced thickness where the amorphous chains in this layer will be presumably closer to a rubberlike state. In this view, the progressive addition of SA on the surface of the PCC particles would leave the polyethylene chains in the interphase layer progressively less disturbed by the presence of the filler. Also the thickness of the interphase would be progressively smaller, thus explaining the progressive decrease in ΔV with increasing SA content, with its effect on the effective volume fraction of the filler particles.

In [31] it was noted that the presence of significant amounts of large agglomerates might also affect the volume strain data, through their effects on the effective volume fraction, by entrapping polymer or even air inside them. During tensile deformation, agglomerate tends to behave as a single large particle. The polymer or the air entrapped in such agglomerate would raise the effective filler content. By

[2] Over the past 15 years, in our laboratory we have measured with this technique the volume deformation of several blends and composites. In the case of polyethylene based polymers—and only with this type of polymers—negative volume strains have always been reported [29]. In the work of Gaucher-Miri et al. [30], the measurements were made until large strains with a video apparatus instead of extensometers. In this way valid data on a low density PE copolymer could be collected even after necking. It is worth noting that the data measured in this work are quite similar to ours, where we measure a volumetric strain of 0.03 for an axial strain of 0.3, although the crystallinity of our pure HDPE is higher—$X_c = 56\%$—compared to the low density PE copolymer studied by the quoted authors—$X_c = 32\%$.

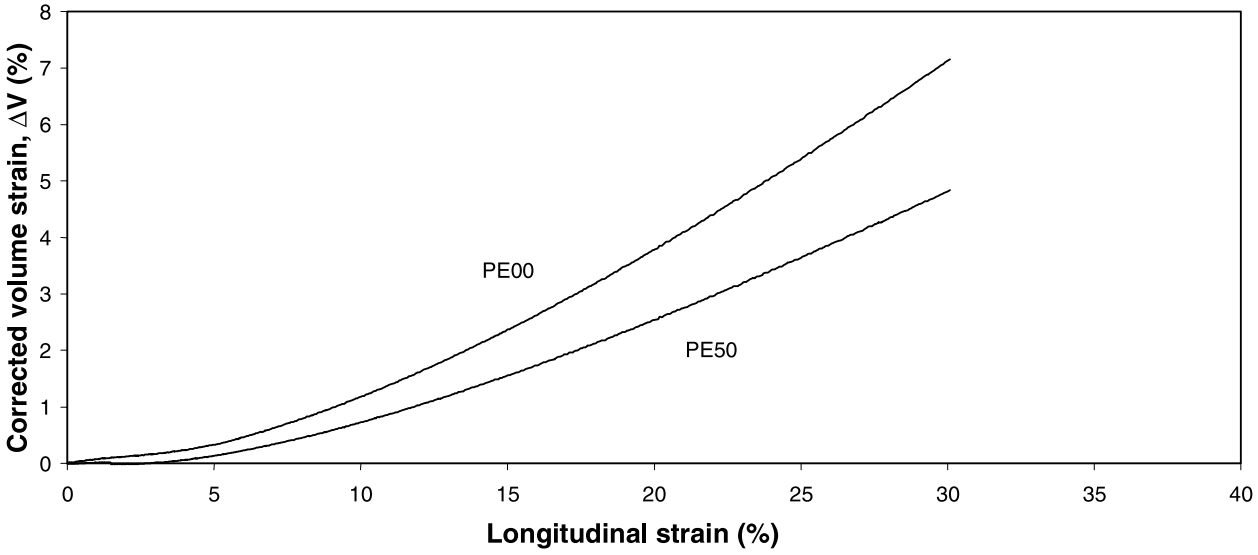

Fig. 6. Volume strain due to void growth, $(\Delta V/V_0)_V$ calculated from Eq. (1), plotted versus longitudinal strain for PE00 and PE50.

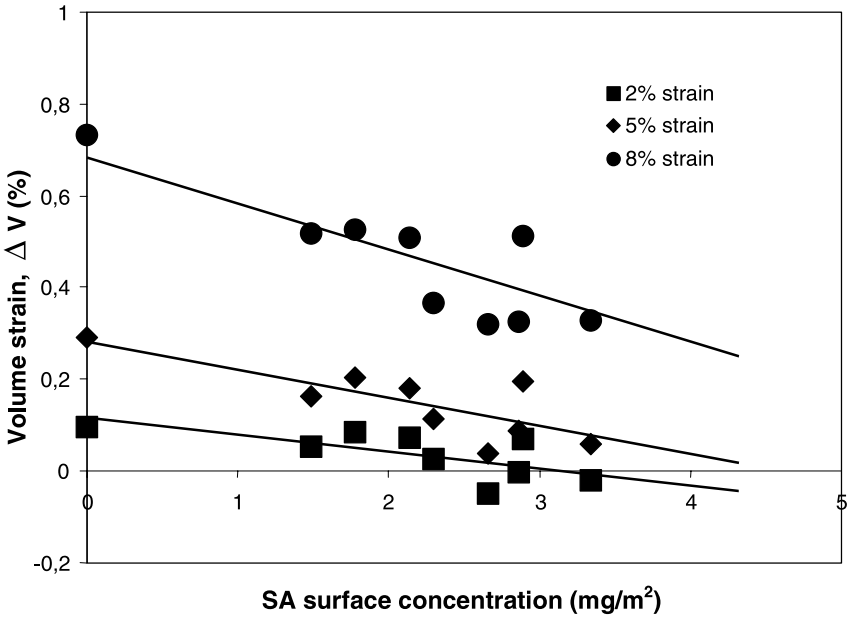

Fig. 7. Dependency of $(\Delta V/V_0)_V$ from SA content at 2, 5 and 8% longitudinal strain.

increasing the SA surface concentration, the number and size of agglomerates progressively decreases so this could also reduce the amount of filler or air trapped into the agglomerates. The overall effect is a decline in the effective volume fraction and a decrease in volume strain.

3.3. Impact strength

Fig. 8 shows the dependency of Impact strength of the composites as a function of the SA content/m^2 of PCC. As it can be noticed, the addition of uncoated PCC to HDPE causes the impact strength to sharply drop from 14.3 to 3.3 kJ/m^2. Progressively adding SA leads to an almost linear increase in toughness within the compositional limits explored[3]. In particular the composite with PCC coated with 4.3 mg/m^2 has an impact strength of 11.7 kJ/m^2, that is only about 20% less than pure HDPE, while the Young's modulus for the same material is increased by almost 50% and yield stress of about 4%.

It should be noted that the fact that coated particles show better fracture behaviour apparently contradicts the idea that

[3] In the second paper in this series fracture resistance data obtained from a new set of materials with larger SA content will be presented. It can be anticipated that composites with PCC particles with a SA coating rate above 5 mg/m^2 show a larger impact strength than pure HDPE.

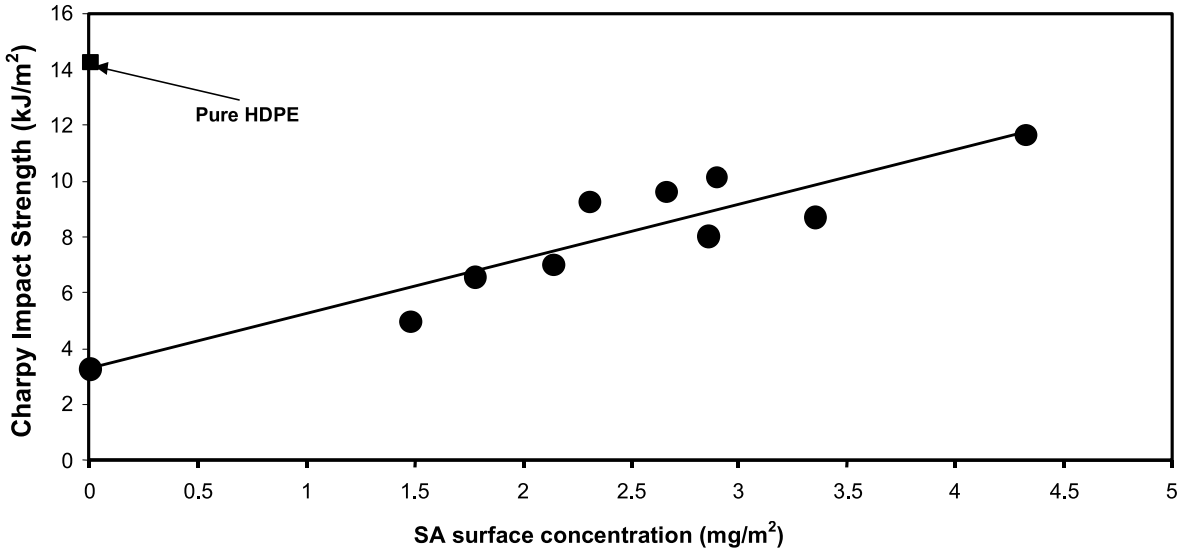

Fig. 8. Dependence of the impact strength of PCC/HDPE nanocomposites upon SA content.

the stearic acid coating is added to facilitate the debonding and void growth process which are necessary elements of the filler toughening process. Thus one would then expect that the composites with coated PCC particles should present a higher volume strain than composites with uncoated particles. A similar problem was found in rubber toughening where blends with bigger particles—which are more brittle—show a larger volume strain than the tougher blends with smaller particles [15–17]. In the case of rubber particles, the strain at cavitation is an inverse function of particle size, with bigger particles cavitating more promptly than smaller particles. In analogy with rubber toughening we can think that bigger particles debond more easily than smaller particles and that if particle–matrix debonding occurs too early—that is when the material is still in its elastic range—the triaxial state of stress at the crack tip will favour matrix crazing and brittle fracture. When instead debonding occurs close to yielding, the dilatant component of the stress tensor enables dilatational plastic straining in the zone ahead the crack tip, leading to ductile fracture. So only composites with 'just-in-time' debonding—i.e. close to yielding—can show high impact resistance. In our context, uncoated particles are more agglomerated—thus bigger—than the coated ones and we can expect too early debonding followed by crazing and brittle fracture.

3.4. Morphological analysis

During tensile tests in toughened HDPE composites, a stress whitening zone develops throughout the length of the neck. Indeed stress whitening is due to the scattering of visible light and can be attributed to the various processes that can take place in the polymer, such as matrix crazing, matrix shear yielding, and filler/matrix debonding. For further elucidation of the mechanism of deformation during tensile tests in HDPE composites, electron microscopy was employed. Figs. 9 and 10 show the cold fractured surfaces of PE00 and PE20, respectively. Some agglomerated particles of a few μm size and elongated voids due to interface debonding in PE00 composites (uncoated PCC) are clearly visible in Fig. 9(a), unlike Fig. 10(a) which shows the cold fractured surfaces of PE20 (PCC coated with nominal 0.2% SA). This is because stearic acid decreases the surface tension reducing the formation of agglomerates during melt compounding. Fig. 9(b) and (c) are close-ups of Fig. 9(a). Many small and big voids due to debonding are observed in these figures. This indicates that cavitation started from the interface and that elongated voids grow along the tensile direction. Besides it can be seen distribution of particles in PE00 is not very good. Fig. 10(b) and (c) are blow-ups of Fig. 10(a). A part from some agglomerated particles, a relatively good dispersion is clearly visible. Besides, it can also be observed that there are many small voids. By comparing Figs. 9 and 10 one may conclude that addition of stearic acid, although does not prevent completely the particles from aggregating, can effectively reduce their size improve dispersibility preventing the creation of very large voids (a more quantitative analysis will be presented in the second part of this communication).

3.5. Calorimetry

DSC thermograms of HDPE and HDPE composites, recorded on cooling, is shown in Fig. 11. The values of the thermal parameters are summarized in Table 5. On heating, a single melting peak is observed for all examined samples, while during cooling from the melt a double exothermic peak is found for the composite with uncoated PCC particles.

Table 4 reports the effects of the SA on the melting point of the materials for the first and the second heating run (T_{mI} and T_{mII}). As it can be observed the addition of 10 vol%

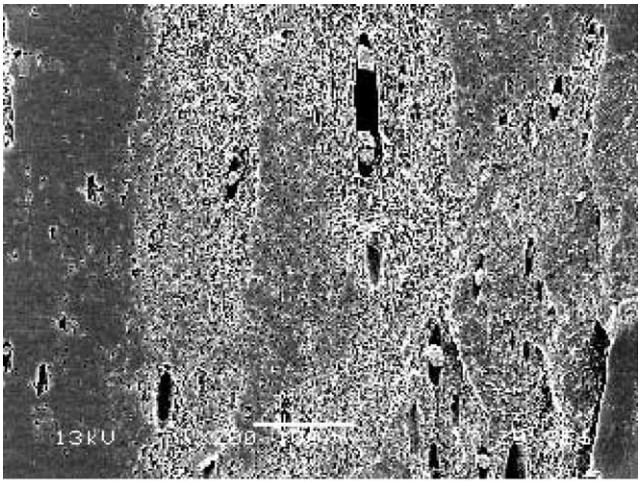

a)

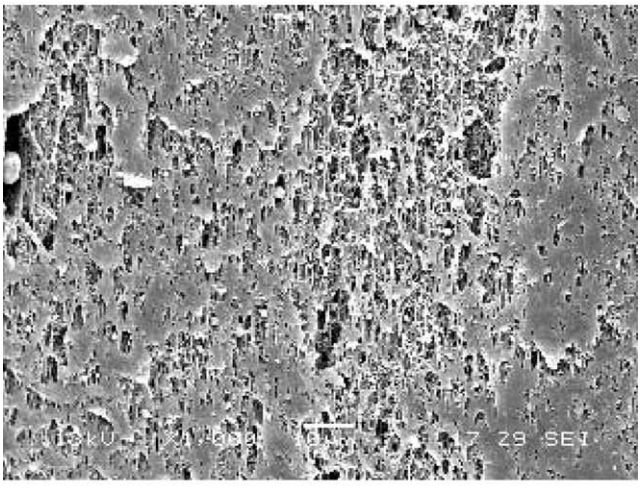

b)

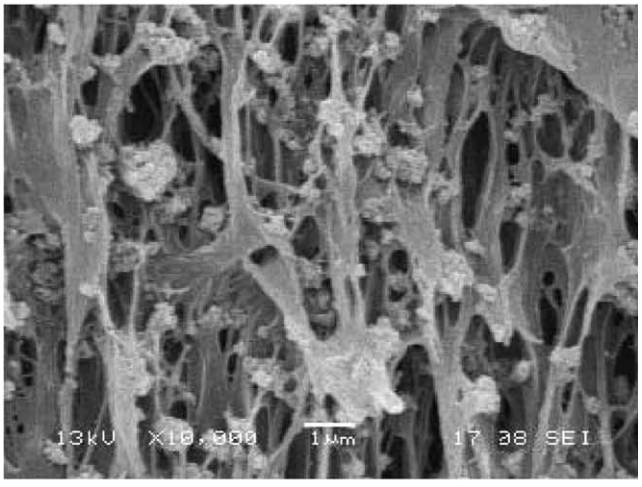

c)

Fig. 9. SEM micrographs of the surface of a tensile specimen of PE00, cold fractured along the draw direction (a) a view of the fracture surface; (b) and (c) are close ups of (a).

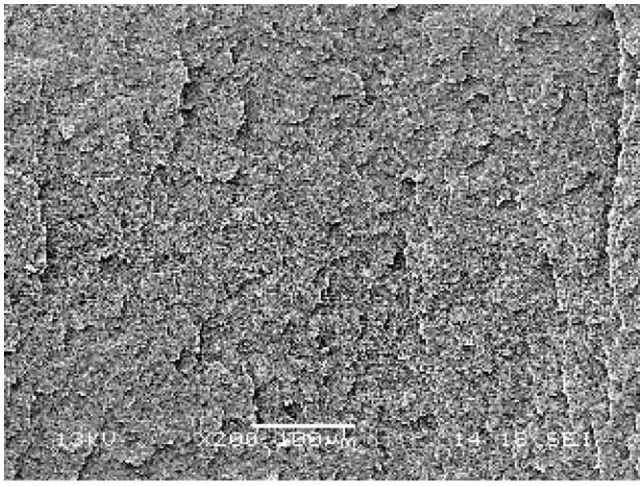

a)

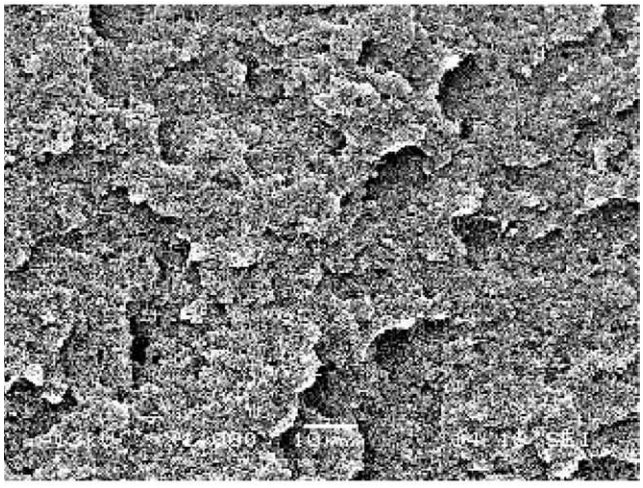

b)

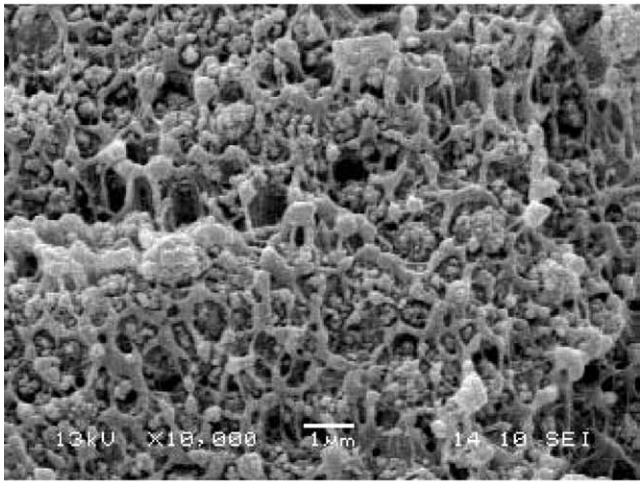

c)

Fig. 10. SEM micrographs of the surface of a tensile specimen of PE30, cold fractured along the draw direction: (a) general view of the fracture surface. Micrographs (b) and (c) are close-ups of figure (a).

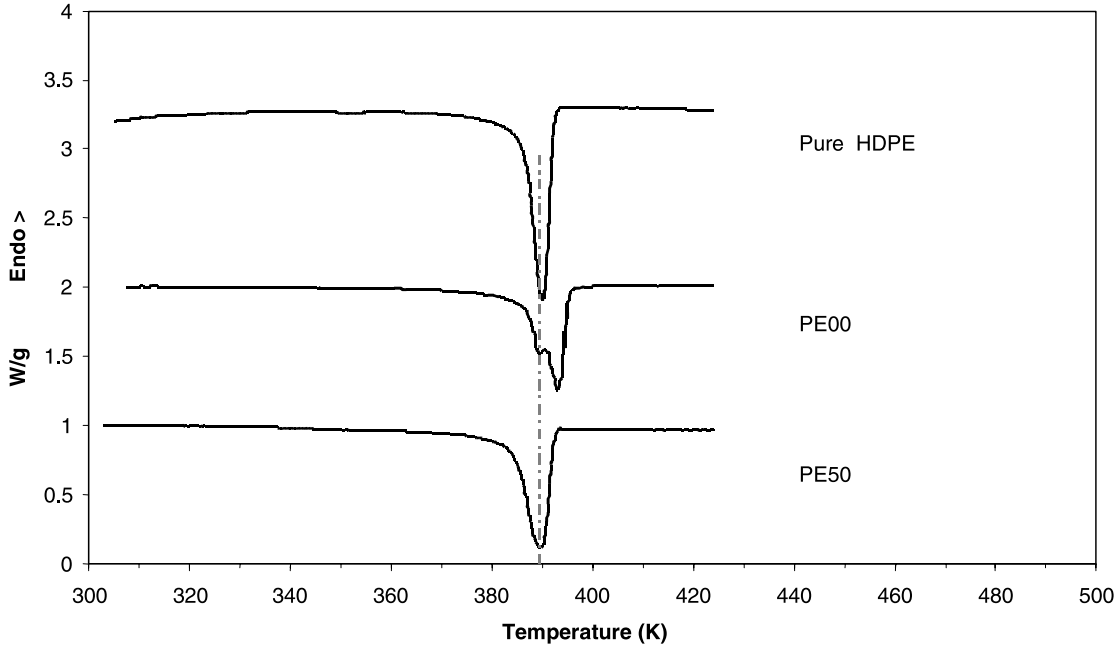

Fig. 11. DSC cooling thermograms for PE00, PE00 and PE50.

PCC to HDPE causes a slight rise in both T_{mI} and T_{mII}. At a SA content of 5 wt%, nominally correspondent to the monolayer concentration, the material shows a not very pronounced maximum in the melting temperature.

In Table 5 are given values of ΔH_{mI} and ΔH_{mII} per gram of polymer as a function of the SA content. As it can be noticed, during both first and second heating runs, the melting enthalpy is practically constant and it seems that the SA has no significant effect on the melting heat of pure HDPE.

The results of crystallisation behaviour of HDPE/10 - vol% PCC as a function of SA content are shown in Fig. 12. The crystallisation temperature T_c is increased for the composite with uncoated $CaCO_3$, compared to the pure HDPE, while PCC/HDPE composites with SA coated particles show the same crystallisation temperature of pure HDPE. A similar behaviour can be noted for the onset temperature, T_O, as a function of SA content. Compared to pure HDPE, the onset temperature for the composite with uncoated $CaCO_3$ is increased by about 3 °C, while the addition of the SA to PCC particle has no significant effect on the onset temperature.

Table. 5 reports ($T_O - T_C$) and crystallization heat values for all composites. These quantities do not show substantial variations for all materials. Moreover Table 5 shows the crystallization heat and the crystallinity index, X_C, of the HDPE matrix in all composites with 10 vol% PCC with varying SA content. The value of X_C is rather constant for all composites, indicating that the SA content on the particles has no influence on the crystallinity of the polymer matrix. The crystallinity index ranges, for all composites, between 71% and 73%, while the corresponding value for pure HDPE is about 56%.

From these results we can say that uncoated $CaCO_3$ has a very weak nucleating effect on the crystallisation of HDPE, while the addition of a SA coating on $CaCO_3$ has no influence on the crystallisation process. In fact the addition of SA obliterates the effect of $CaCO_3$. This can be explained by the fact that when the surface of $CaCO_3$ is coated by SA, which is chemically very similar to polyethylene, the interactions between the filler surface and the matrix substantially decrease and the particles do not show to behave as nucleating agents.

3.6. Rheological analysis

The log–log plots of apparent shear viscosity η versus apparent shear rate γ for all composites and for pure HDPE are shown in Fig. 13. Curves 2–11 have been progressively shifted of a factor 0.5 along the log (shear rate) axis for clarity. All materials showed a shear thinning behaviour: the value of viscosity decreases with increasing shear rate. The bilogarithmic plots are based upon the Power Law model [32]:

$$\eta = k\,\gamma^{n-1} \text{ hence } \log \eta = \log k + (n-1)\log \gamma \qquad (5)$$

where k is the consistency index and n the Power Law index.

Fig. 13 shows that the materials studied in this work, including the pure HDPE, follow a Power Law relationship at low apparent shear rates. Table 5 reports the Power Law indexes for all materials in the low shear rate regime, i.e. the 'linear' region in the bilogarithmic plot. As it can be observed, the Power Law Index, n, is approximately constant when 10 vol% PCC are added to HDPE, irrespective of SA content. The consistency index varies from 0.93

Table 5
Calorimetric data for PCC/HDPE composites

HDPE Compounds	ΔH_{mI} (J/g of HDPE)	ΔH_{mII} (J/g of HDPE)	$-\Delta H_c$ (J/g of HDPE)	X_c (HDPE)	T_{mI} (°C)	T_{mII} (°C)	T_c (°C)	T_O (°C)	$T_O - T_c$ (K)
Pure HDPE	165.43	196.83	183.22	0.56	128.59	131.40	116.91	119.08	2.17
PE00	208.22	227.50	211.44	0.71	129.93	131.84	119.93	122.18	2.25
PE20	209.38	227.38	201.77	0.71	128.99	131.31	116.60	118.81	2.21
PE30	210.41	230.67	204.94	0.72	129.36	131.26	117.16	119.16	2.00
PE38	204.57	227.93	204.14	0.70	129.53	131.56	116.72	118.99	2.27
PE45	209.80	224.83	213.45	0.72	129.71	131.96	116.52	119.15	2.63
PE50	207.00	225.62	217.83	0.71	131.14	132.57	116.47	119.22	2.75
PE55	206.52	228.84	215.15	0.70	130.74	132.49	117.16	119.79	2.63
PE60	212.78	230.00	209.62	0.73	129.37	132.15	117.45	119.79	2.34
PE70	211.20	226.59	209.13	0.72	129.57	131.46	117.41	119.67	2.26
PE90	207.55	229.02	216.43	0.71	130.51	132.51	116.75	119.49	2.74

for pure HDPE to 1.46 for PE00 and remains more or less around this value for all composites with coated PCC particles.

The degrees of linearity in the log–log plot at high shear rates varies with SA content. Particularly the composite with uncoated $CaCO_3$ particles shows a more marked decrease in apparent shear viscosity at high shear rate respect to the low shear rate regime. This is normally attributed to a breakdown of the agglomerate structure of $CaCO_3$ particles [33]. It is known that liquid binding or immobilization mechanisms can dominate the rheological characteristics of polymer suspensions. Chemisorbed or physisorbed bound polymer molecules can be present on the particle surface or free liquid polymer immobilized within the inner voids and capillaries of the particle aggregates. In particular, the polymer chains trapped inside the voids of the aggregates are actually excluded from contributing to the continuous fluid phase flow. These polymer molecules can be regarded as 'hydrodynamically immobilized' by the aggregates. The liquid fraction undergoing this type of (inner) volume immobilization has to be regarded as a contribution to the disperse phase with the effect of raising the effective filler volume fraction. At each shear rate there will be a structural equilibrium between the aggregation and deaggregation tendency so the effective volume fraction will be a function of shear rate. For this reason the measured viscosity of the blend will decrease with shear rate, thus showing a shear thinning behaviour.

In this contest, the composite with no surfactant can be expected to behave as if its volume fraction was actually larger than for those coated with a surface agent. Also the composite with coated PCC will show a less marked shear thinning behaviour because the surfactant prevents the formation of large agglomerates by decreasing the surface tension between the matrix and filler [21].

In Fig. 14 the dependency of viscosity from SA content in HDPE/10% vol. $CaCO_3$ composite at different piston speeds are shown. As expected the addition of $CaCO_3$ (with or without surfactant) causes a rise in viscosity respect to pure HDPE. The increase in viscosity is more marked for uncoated $CaCO_3$ due to a larger interference with the polymer flow. Also the increase in viscosity is less marked at high velocity (Table 6).

The addition of SA causes a decrease in viscosity, with respect to the value of the HDPE/uncoated $CaCO_3$ composite. It can be expected that raising SA content causes a drop in the level of interactions between particles, reducing the amount and the average size of agglomerates, and improves the distribution of the particles in the matrix. It has been observed, however, that in several systems a reduced particle size causes an increase in apparent viscosity [33]. So the decrease in viscosity noticed in this work may be due to a reduction of the immobilized polymer fraction because of the lower interfacial tension between the solid particles and surrounding liquid phase when a surfactant layer is present. Another effect of the surface

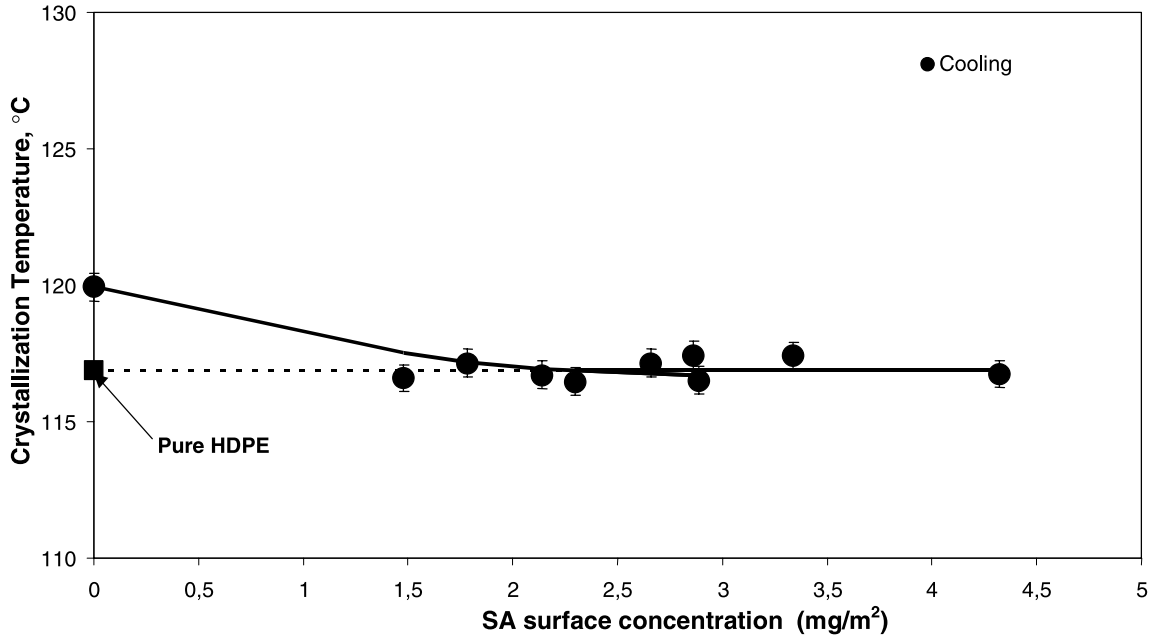

Fig. 12. Dependency of crystallization temperature of 10 vol% PCC/HDPE composites on SA content.

agent, by reducing the size of agglomerates, is to decrease the effective solid volume fraction and thus the apparent viscosity. This might also explain the behaviour shown in Fig. 13. With increasing SA content, especially at low speed, the viscosity progressively decrease up to a threshold value of 5% which corresponds to the formation of a theoretical stearic monolayer around the $CaCO_3$ particles. This indicates that super-monolayer coatings do not seem to contribute in reducing the apparent viscosity of the compounds.

4. Discussion

The impact tests reported in this work have shown that the addition of uncoated PCC to HDPE causes a sharp drop in impact strength of the composite. Also it was shown that progressively adding SA to PCC particles leads to an almost linear increase in toughness, without a substantial parallel loss in Young's modulus and yield stress. It can be noted that the SA coating levels used in this work we obtain only an improvement without fully recovering the loss of

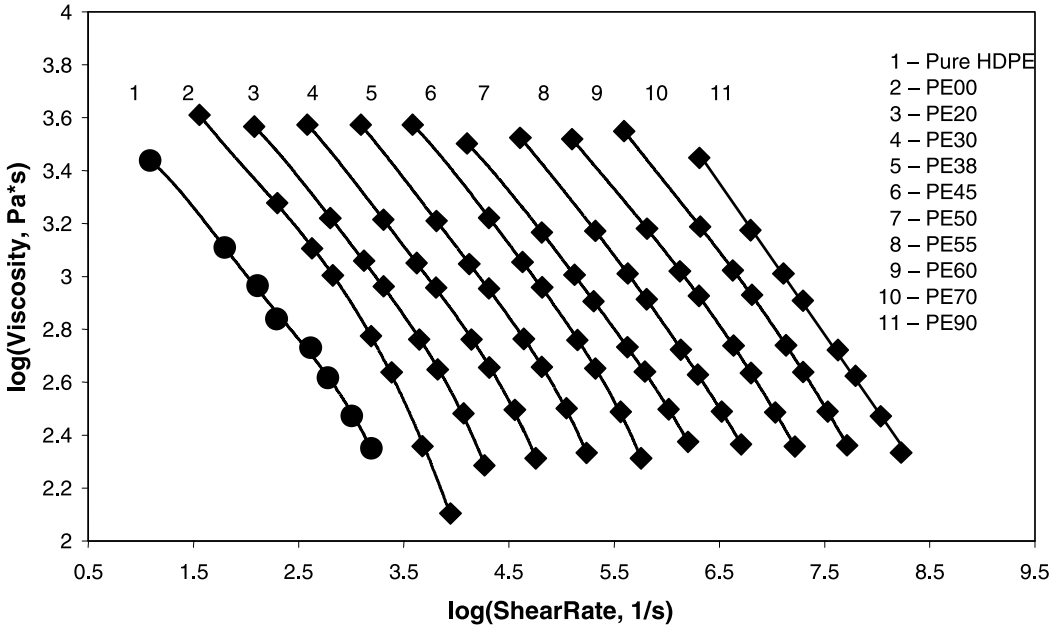

Fig. 13. Viscosity versus shear rate of pure HDPE and 10 vol% PCC/HDPE composites. Curves 2–11 have been shifted of a factor 0.5 along the log (shear rate) axis for clarity.

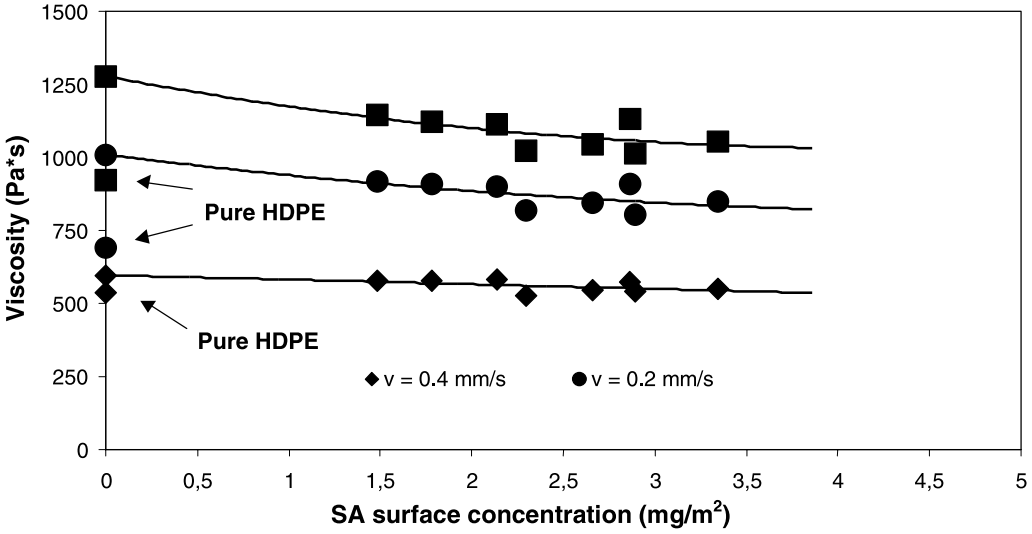

Fig. 14. Variation of viscosity for 10 vol% PCC/HDPE composites versus SA surface coverage.

toughness due to the addition of uncoated PCC particles, thus questioning the concept of filler toughening HDPE with nanoparticles. In the next paper in this series, though, it will be shown that composites with PCC particles with a SA surface concentration above 5 mg/m^2 show a larger impact strength than even pure HDPE.

The microscopical analysis carried out on composites obtained from both uncoated and coated PCC showed cavities and voids due to debonding and deformation bands in the stress whitened areas, suggesting that the deformation mechanism is basically the same. The main difference observed on the fracture surface is the dependency of the size of agglomerated particles from stearic acid content. Although the addition of stearic acid cannot completely prevent the formation of agglomerates the main effect of this surface agent is to effectively reduce their size, thus leading to a more ductile behaviour.

Argon and Cohen [4–7] have explained the toughening effect of $CaCO_3$ in HDPE in term of crystal plasticity by assuming the presence of an oriented PE lamellae preferentially grown against $CaCO_3$ surfaces. Their study

Table 6
Power Law constants for PCC/HDPE composites

HDPE Compounds	Power Law index (n)	Consistency index (k, Ns^n/m^2)$\times 10^4$
Pure HDPE	0.52	0.93
PE00	0.50	1.46
PE20	0.49	1.33
PE30	0.47	1.44
PE38	0.47	1.45
PE45	0.47	1.47
PE50	0.50	1.17
PE55	0.47	1.33
PE60	0.48	1.27
PE70	0.47	1.40
PE90	0.45	1.47

[5] on the morphology and orientation of HDPE in sub-micron thickness films grown on $CaCO_3$ and crosslinked ethylene–octene rubber substrates, carried out by using combined WAXS measurements and AFM imaging, lead to the conclusion that, for films of thickness less than 0.3 μm, lamellar crystallites preferentially grow 'edge-on', in a sheaf-like morphology, on the calcite or rubber interfaces with the (100) crystallographic planes of the lamellae lying parallel to the interfaces, while in films thicker than 0.4 μm, the spherulitic morphology becomes dominant. This change in morphology and crystalline orientation has been attributed by these authors [5] to accelerated secondary nucleation on the layer of lamellae formed adjacent to the substrate, resulting in oriented 'edge-on' growth, parallel to this surface. In this hypothesis, low energy and low shear resistance crystallographic planes orient themselves parallel to particle/matrix interfaces during crystallisation. After debonding, for these preferentially arranged crystals, the highly deformable, lower plastic resistance slip planes lie parallel to the interface, thus parallel to the direction of maximum shear force. This advantageous crystal location would be ideal for prompting a rapid stretching of the ligaments among debonded filler particles since it enables to significantly reduce the high energy barrier required to be surmounted to activate the complex plastic deformation process implied for the transformation of the interface lamellae into crystalline fibrils oriented parallel to the principal strain direction.

Argon and Cohen [4–7] also suggested that when the ligament thickness (interparticle distance) is larger than a critical value roughly corresponding to twice the oriented crystallisation layer, the preferentially oriented interface lamellae no longer percolates through the material. In this case, the randomly oriented crystallites formed by secondary nucleation on the oriented lamellae layer present a significantly higher plastic resistance, leading to a serious

reduction in the shear deformation rate. The amount of energy dissipated in the damage zone near the crack tip is severely limited and the material tends to exhibit a brittle behaviour.

The calorimetric data discussed in this work show however several elements of contrast with the toughening mechanism suggested by Argon and Cohen [4–7]. It was in fact shown that the uncoated PCC particles have a very small nucleating effect on HDPE, which is not what one would expect in the case of a preferential growth of PE crystals on the surface of PCC particles. The stearic acid content had no influence on the melting temperature or crystallinity of the PE phase. The dependence of the crystallization and onset temperatures versus SA surface concentration is—in this regard—particularly illuminating. While the sample filled with uncoated PCC shows a larger value compared to the unmodified matrix, all samples with PCC treated with SA at various surface concentrations, show identical values of T_C and T_O with respects to that of the unfilled HDPE, at least within experimental error.

If the mild nucleation effect found for the uncoated PCC particles supports the view that a preferential interface-induced organisation occurs during crystallisation of the macromolecules near the PCC/HDPE interface, our results also show that this nucleating effect is reduced to an almost insignificant level when the PCC particles are coated with SA.

This can be explained with the role of the interphase present in the molten state around each particle during crystallization. In our work we have explored a range of SA surface coating from 0 to 4.32 mg/m^2, corresponding to almost two times that nominally required for a monolayer. In fact, Rothon has reported that the formation of a dense packed layer of stearate molecules—a self-assembled 'monolayer'—requires 0.25 wt% of stearic acid for each m^2/g of calcium carbonate surface, i.e. 2.5 mg/m^2 [2–3]. This figure has been calculated from the number of calcium ions present on the surface, with the aliphatic chains of the acid oriented perpendicular to the surface and restricted in their motion, and corresponds to about 0.21 nm^2/molecule. Suter et al. [19] have also suggested that the alkyl tails in the stearic acid chemisorbed monolayer form an ordered solid-like phase similar to those found in liquid-crystals.

By employing a quantity of stearic acid in excess to that required to complete the surface reaction with the calcium cations leads to formation of a bilayer or even of a multilayer. In the case of a bilayer, only the molecules arranged in the first layer are chemisorbed on the surface, while the excess molecules form a physisorbed second layer [19]. The molecules in the chemisorbed and physisorbed layer are intercalated with the alkyl groups arranged in a tail-to-tail assembly which leaves the carboxyl groups of the second layer molecules sticking out of the organic bilayer [19]. Osman and Suter [23] suggested that calcium stearate is present as a heterogeneous particulate phase in low density polyethylene (LDPE) to explain the reinforcing effect on the stiffness of over-coating the calcium carbonate filler. Other properties like tensile strength, yield strain and ultimate elongation, on the contrary, showed a reduction. This hypothesis does not seem to hold in our case since the stiffness is progressively lowered while the impact strength grows on increasing the excess of surfactant. So it seems more likely that even in the ideal case that a perfect monolayer might be formed around the particles, the excess SA coating probably forms a bilayer of calcium stearate tails intermeshed (interpenetrating) with polyethylene chains.

The assumption is reasonable since the stearic tail is basically a short chain of methylene units, thus practically indistinguishable, on the atomistic level, from higher molecular weight PE chains. When cooling from the molten state, after being injected in the mould, the polyethylene molecules are not in direct contact of the $CaCO_3$ surface but only with the organic interlayer formed by the mobile lipophile ends of the SA chains. It is clear that the nucleating effect of the substrate surface is strongly diminished as we experimentally found in this work. As a consequence the formation of a transcrystalline layer is questionable, since the surface tension is dramatically reduced.

Argon and Cohen [4–7] showed that, for the preferentially crystallised layer, the low plastic resistance (100) planes are oriented parallel to the direction of maximum shear strain thus leading to an easier stretching of the ligaments between cavitated particles. In our work we have observed that the addition of 10 vol% of uncoated PCC to HDPE leads to an increase in yield stress and Young's modulus. Also the volume measurements show early debonding and volume expansion for this composite. This is consistent with the formation of a rigid interphase. In fact, in the presence of the debonding of the particles from the matrix, it would be reasonable to expect a reduction of a factor $(1-\phi)$ in yield stress, while the experimental value for uncoated PCC/HDPE composites is about 10% higher than that of the pure HDPE polymer. It thus appears that these crystals are less mobile than for pure HDPE. Our calorimetric data show a small nucleating effect of the uncoated PCC particles, in agreement with the formation of a transcrystalline layer with the more easily deformable (100) planes oriented parallel to the particle–matrix interface, as stated by Argon and Cohen [4–7]. The two observations suggest the conclusion that we are in presence of two conflicting tendencies: on one side the nucleating effect of the $CaCO_3$ particles enables the formation of crystals with low resistance planes oriented parallel to the particle surface, leading to a softener interface; on the other side the amorphous HDPE molecules adsorbed on the surface are substantially less mobile than those in the bulk resulting in a stiffer interphase. From our mechanical data it seems that the stiffening effect is larger than the softening one.

Several authors have in fact suggested the formation of an 'immobilised polymer layer' with reduced molecular mobility at the particle–matrix interphase causing a more

brittle behaviour [2,3,34,35]. This has conflicting consequences on the properties of the interlayer in semicrystalline polymers. If the presence of the filler particles may provide solid surfaces as heterogeneous nuclei for crystallisation, the reduced mobility of the chains, on the other hand, hinders the growth of crystals. This can lead to the formation of small, imperfect crystallites or even to an almost amorphous interlayer. The composite will have a larger deformability albeit with a lower stiffness and tensile strength [36]. So the balance between stiffening and softening effects is often decided by the level of interfacial adhesion.

Thus the question that is still opened is which type of interphase will form when a hydrophobic coating is present at the surface of a filler and which effect can have on the properties of the composite. The structure and properties of such an ultrathin organic film should have a strong influence on the final properties of the composites because this hydrophobic coating determines not only the particle-particle and the particle–matrix interactions but also determines the buildup of the interphase. Moreover, the properties of the interphase are particularly important for nanocomposites where a large volume fraction of the polymer matrix belongs to or is affected by the interphase layer, with properties very different from those of the bulk polymer.

If this is a reasonable description of the interphase for the PCC/HDPE nanocomposites studied in this work, a higher mobility is to be expected by increasing SA surface concentration. In fact, when a calcium fatty acid salt is present on the surface, PE molecules are not more adsorbed directly on the surface, forming an immobilised rigid layer, but they are intermeshed with the alkyl tails of stearate molecules bonded with only weak Van der Waals forces.

Thus one would expect that when SA is added, both E and σ_y decrease. This is supported from our experimental results of Figs. 3 and 4, which show a continuous reduction of these properties until a plateau level is attained, from SA $\sim$ 2,7 mg/m^2. This roughly corresponds to the nominal monolayer coating.

This hypothesis of a progressively softer interphase could also explain the reduced volume change observed on increasing SA content. In the case of uncoated PCC we have a rigid and thick interphase strongly bonded to the particles. When strained up to a critical value, debonding will occur followed by microvoid expansion. Upon adding SA a progressively softer and thinner interphase builds up with PE molecules and crystals bonded to alkyl tails by weak forces. When strained, this interphase might more easily accommodate shear deformations of the crystals near the interface and debonding is retarded. Also we observe from Fig. 6, where the volume strain for PE00 and PE50 is plotted versus longitudinal strain, the slope of volume evolution curve for the composite with uncoated particles is larger than that for coated particles (0.257 and 0.141, respectively). In a previous paper we have shown that the presence of an immobilized interphase or of agglomerates can have an effect on the slope of the volume evolution curve by raising the effective volume fraction of the particles [31]. The SEM analysis has shown that the number of agglomerates and their average size progressively decreases with SA content, although for coated PCC composites the extremely large agglomerates present in PE00 have not been observed. In any case, the variation of the degree of agglomeration with SA and the limited number of very large agglomerates in PE1000, does not appear so dramatic to determine a very large difference in the effective volume fraction between the composites with coated and uncoated PCC. This view is supported also by the rheological analysis. Thus the observed change in slope of the volume strain-elongation curve between coated and uncoated PCC/HDPE composites seems consistent with a thinner interphase when the particles are coated with SA, although the quantitative morphological analysis that will be presented in the second part of this communication will enable to more accurately assess this issue.

5. Conclusions

In order to investigate the role of SA content on tensile properties and in volume evolution during stretching of PCC/HDPE composites, a series of HDPE/10 vol% PCC composites with different SA content were prepared. Tensile tests were carried out at room temperature and different strain rates. The results show that the addition of 10 vol% calcium carbonate to HDPE causes a rise in Young's modulus and yield stress of its composites but does not change the tendency of the material to neck and draw. The addition of SA has the effect of decreasing both Young's modulus and yield stress of the composites compared to the uncoated PCC composites. During the tensile test filled HDPE composites showed stress whitening zones appear and develop along the gauge length.

The results of volume change measurements during stretching showed that for all composites it can be observed an increase of volume strain with deformation, due to the debonding phenomenon, while pure HDPE showed actually a decrease in volume with elongation. At constant deformation, for the composites with coated PCC, it can be observed that an increase in the SA content leads to a decrease in volume change; this is due to the influence of SA on the debonding phenomenon, decreasing the slope of the volume strain-elongation curve.

The microscopical evaluation showed cavities and voids due to debonding and deformation bands in the stress whitened areas. This confirms that the origin of the volume evolution is due to void initiation and growth. A dependency of the size of agglomerated particles from stearic acid content was observed. The addition of stearic acid cannot completely prevent the particles from aggregating but it can reduce the size of the agglomerates.

The results of DSC tests show that the addition of 10 vol% uncoated calcium carbonate to HDPE causes a very slight rise in both T_{mI} and T_{mII}. For composites with SA coated particles no significant effect on the melting temperature has been observed.

Viscosity tests have been carried out using a capillary rheometer. The results of this analysis are the addition of uncoated PCC causes a rise in viscosity, although this increase is less marked at high shear strains. The addition of SA causes a decrease in viscosity, with respect to the value for the uncoated PCC/HDPE composite. Above a SA surface concentration of 2.5 mg/m^2, corresponding to the theoretical monolayer composition, a plateau value of viscosity is achieved.

The addition of 10 vol% calcium carbonate to HDPE causes a sharp drop in impact strength. The addition of SA has the effect of progressively increasing the impact strength of the composites compared to the uncoated PCC composites.

Acknowledgements

The authors wish to acknowledge the collaboration of Mr Balducci of Interplast, Scandicci (FI), Italy for the injection moulding of all materials used in this work.

References

[1] Bucknall CB. Toughened plastics. London: Applied Science; 1977.
[2] Rothon RN, editor. Particulate-filled polymer composites. Harlow: Longman Scientific and Technical; 1995.
[3] Rothon RN. In: Jancar J, editor. Mineral fillers in thermoplastics: filler manufacture and characterisation. Mineral fillers in thermoplastics I. Raw materials and processing. Advances in polymer science, vol. 139, 1999. p. 67.
[4] Argon AS, Bartczak Z, Cohen RE, Muratoğlu OK. Novel mechanisms of toughening semi-crystalline polymers. In: Pearson RA, Sue HJ, Yee AF, editors. Toughening of plastics, advances in modeling and experiments, Symposium series 759. Washington, DC: ACS; 2000. p. 98.
[5] Bartczak Z, Argon AS, Cohen RE, Weinberg M. Polymer 1999;40: 2347.
[6] Wilbrink MWL, Argon AS, Cohen RE, Weinberg M. Polymer 2001; 42:10155.
[7] Thio YS, Argon AS, Cohen RE, Weinberg M. Polymer 2002;43:3661.
[8] Fu Q, Wang G. Polym Eng Sci 1992;32:94.
[9] Levita G, Marchetti A, Lazzeri A. Polym Compos 1989;10:39.
[10] Wu S. Polymer 1985;26:1855.
[11] Broutman LJ, Shau S. Mater Sci Eng 1971;8:98.
[12] Lange FF, Radford KC. J Mater Sci 1971;6:1197.
[13] Lange FF. Phil Mag 1970;22:983.
[14] Lange FF. J Am Ceram Soc 1971;54:614.
[15] Lazzeri A, Bucknall CB. J Mater Sci 1993;28:6799.
[16] Lazzeri A, Bucknall CB. Polymer 1995;36:2895.
[17] Lazzeri A, Bucknall CB. Recent development in the modelling of dilatational yielding. In: Pearson RA, Sue HJ, Yee AF, editors. Toughening plastics, advances in modeling and experiments, Symposium series 759. Washington, DC: ACS; 2000. p. 14.
[18] Zuiderduin WCJ, Westzaan C, Huétink J, Gaymans RJ. Polymer 2003;44:261.
[19] Osman MA, Suter UW. Chem Mater 2002;14:4408.
[20] Pukánszky B. In: Karger-Kocsis J, editor. Polypropylene: structure, blends and composites. London: Chapman and Hall; 1995. Chapter 1.
[21] Haworth B, Raymond CL, Sutherland I. Polym Eng Sci 2001;41:1345.
[22] Keller DS, Luner P. Colloids Surf A: Physicochem Eng Aspects 2001; 161:401.
[23] Osman MA, Atallah A, Suter UW. Polymer 2004;45:1177.
[24] Thio YS, Argon AS, Cohen RE. Polymer 2004;45:3139.
[25] Wunderlich B. Macromolecular physics. vol. 3. New York: Academic Press; 1980.
[26] Suwanprateeb J, Tiemprateeb S, Kangwantrakool S, Hemachandra K. J Appl Polym Sci 1998;70:1717.
[27] Mlecnik E, la Mantia FP. J Appl Polym Sci 1997;65:2761.
[28] Demjen Z, Pukanszky B. Polym Compos 1997;18:741.
[29] Levita G, Lazzeri A, Butta E, Frosini V. Mater Eng 1989;1:233.
[30] Gaucher-Miri V, Depecker C, Séguéla R. J Polym Sci: Part B, Polym Phys 1997;35:2151.
[31] Lazzeri A, Thio YS, Cohen RE. J Appl Polym Sci 2003;91:925.
[32] Haworth B, Raymond CL, Sutherland I. Polym Eng Sci 2000;40:1953.
[33] Hornsby PR. In: Jancar J, editor. Rheology, compounding and processing of filled thermoplastics. Mineral fillers in thermoplastics I., raw materials and processing. Advances in polymer science, vol. 139, 1999. p. 155.
[34] Maiti SN, Sharma KK. J Mater Sci 1992;27:4605.
[35] Jancar J, Kucera J. Polym Eng Sci 1990;30:707.
[36] Pukánszky B, Fekete E. In: Jancar J, editor. Adhesion and surface modification. Mineral fillers in thermoplastics I. Raw materials and processing. Advances in polymer science, vol. 139, 1999. p. 109.